

OXYGEN SATURATION MEASUREMENTS OF BLOOD IN RETINAL VESSELS DURING BLOOD LOSS

Matthew H. Smith,[†] Kurt R. Denninghoff,[‡] Lloyd W. Hillman,[†] and Russell A. Chipman[†]

[†]The University of Alabama in Huntsville, Department of Physics, Huntsville, Alabama 35899;

[‡]The University of Alabama at Birmingham, Department of Emergency Medicine, Birmingham, Alabama 35226

(Paper JBO-160 received Jun. 18, 1997; revised manuscript received Jan. 5, 1998; accepted for publication Jan. 28, 1998.)

ABSTRACT

We describe a noninvasive technique and instrumentation for measuring the oxygen saturation of blood in retinal arteries and veins. The measurements are made by shining low-power lasers into the eye, and scanning the beams across a retinal blood vessel. The light reflected and scattered back out of the eye is collected and measured. The oxygen saturation of blood within the vessel is determined by analyzing the vessel absorption profiles at two wavelengths. A complete saturation measurement can be made in less than 1 s, allowing real-time measurement during physiologic changes. The sensitivity of this measurement technique to changes in retinal saturation has been demonstrated through a series of pilot studies in anesthetized swine. We present data indicating that retinal venous oxygen saturation decreases during ongoing blood loss, demonstrating a potential application of an eye oximeter to noninvasively monitor blood loss. © 1998 Society of Photo-Optical Instrumentation Engineers. [S1083-3668(98)01403-8]

Keywords oximetry; retina; eye; blood loss; noninvasive monitoring.

1 INTRODUCTION

Early detection of internal bleeding during trauma resuscitation could significantly improve the outcome of a patient's condition.¹ Unfortunately, traditional vital signs such as pulse rate and blood pressure are insensitive indicators of ongoing blood loss.^{2,3} As a result, trauma victims presented to the emergency department may die when physicians are unable to identify internal bleeding, or may require costly and invasive surgery to determine if bleeding is present.

There presently are technologies that can monitor blood loss in the hospital setting. For example, fiber optic catheters can be threaded through the heart and into the pulmonary artery to measure the amount of oxygen in the mixed venous blood (recall that the pulmonary artery carries deoxygenated venous blood from the heart back to the lungs). Arterial blood oxygenation, measured through blood gas analysis or pulse oximetry, gives a supply-side measure of how well the lungs are oxygenating the blood. However, mixed venous blood oxygenation represents a demand-side measure of how much of the available oxygen is being used by the body. As a patient loses blood, and thus loses oxygen carrying capacity, the mixed venous oxygen saturation is known to decrease. From these mixed venous measurements, physicians can determine if a patient is bleeding.¹ Unfortunately, it is logistically difficult to

insert these catheters in an ambulance or during the early period of emergency care. Therefore, a need exists for a technology that could make quick and noninvasive (i.e., without entering the body or puncturing the skin) measurements of blood loss.²⁻⁶

Previous noninvasive techniques for monitoring blood loss have been attempted, but each approach had associated weaknesses. Near-infrared spectroscopy is potentially erroneous due to differences in skull and scalp thickness that alter the optical path length.⁷ Transcutaneous oxygen saturation measurements are made at peripheral vascular beds and have not been widely accepted despite data suggesting sensitivity to early blood loss.⁸ Conjunctival pO_2 measurements have demonstrated sensitivity to blood loss in animal exsanguination studies similar to this study.⁹ The conjunctival oximeter is somewhat invasive, however, as it requires a probe to be placed directly on the conjunctiva of the patient's eye.¹⁰ While a significant need exists for an accurate blood loss monitor, the lack of acceptance of each of these technologies emphasizes that such a monitor must be truly noninvasive, must monitor a central perfusion bed, and must be easy to use.¹¹

The arteries and veins of the retina can be directly imaged through the pupil of the eye, and they are not obscured by thick layers of highly scattering tissues. Additionally, studies have shown that the metabolism and perfusion of the retina and of the cerebrum are similar across a range of normal and

Address all correspondence to Matthew H. Smith. E-mail: SmithMH@email.uah.edu

adverse conditions.¹²⁻¹⁴ The optical accessibility of the retina, coupled with the preservation of retinal circulation during early stages of shock, has led to the hypothesis that retinal venous oxygen saturation may be a valuable parameter for monitoring blood loss.^{15,16}

To investigate this hypothesis, we are developing an instrument called the eye oximeter (EOX).^{17,18} The EOX shines low-power lasers into a subject's eye. The laser beams are scanned across the veins and arteries lying on the retina, and the light that scatters back out of the eye is collected and analyzed. These scans are made at multiple wavelengths, allowing spectroscopic determination of the oxygen saturation of the blood contained in the vessels. Experiments in swine have demonstrated the ability of the EOX to measure the oxygen content of blood in retinal arteries and veins. This article details the instrumentation and signal processing used to make these measurements, and reports the results of animal studies intended to calibrate the EOX¹⁹ and determine the effect of blood loss on retinal venous oxygen saturation.¹¹

2 THE EYE OXIMETER INSTRUMENTATION

Previous retinal vessel oximeters²⁰⁻²² developed by other investigators have been based on modified fundus cameras. These instruments either exposed photographic film at multiple wavelengths or scanned slits of filtered light across retinal vessels. While each of these techniques demonstrated sensitivity to changes of oxygen saturation in human subjects, to the best of our knowledge, the eye oximeter is the first such instrument to be used in an animal model of blood loss. The EOX is a portable device (30×30×12 cm) tethered to an electronics package and laptop computer. The EOX is mounted on a slit lamp base that allows it either to be translated across the cornea and pivoted about the pupil of an immobilized eye or to be used with a fixation target on a cooperative patient.

The EOX instrumentation measures the transmittance of retinal blood vessels at multiple wavelengths. These measurements are then used to calculate the oxygen saturation of blood within the retinal arteries and veins. To achieve this goal, we established a number of design criteria for a prototype instrument. The ultimate requirement, of course, is that the measurement must cause no harm to the patient. Furthermore, the optical system of the EOX should provide a view of the subject's retina to the operator, shine lasers into the eye and scan them across the veins and arteries of the retina, and collect and measure the laser light reflected and scattered back out of the eye. Additionally, data reduction algorithms must analyze the collected scans to determine the percent transmittance of blood within the scanned vessels, and calculate the oxygen saturation of the blood from these measured transmittances. Finally, the eye of

the subject should not need to be chemically dilated, the scans should be fast enough to minimize problems associated with eye movements, and the instrument should accommodate for a range of patient refractive errors. An operational prototype was constructed in accordance with these goals. The device was tested and shown to measure changes in retinal oxygen saturation. The implementation of each subsystem is considered below.

Figure 1 contains a schematic of the eye oximeter breadboard. In Figure 1, all planes marked *r* are conjugate with the subject's retina, and all planes marked *p* are conjugate with the pupil of the subject's eye. A small, 6 V incandescent lamp (IL) and a series of two lenses illuminate a ~2 mm diam circular area of the subject's retina. An image of the lamp filament (1 mm×4 mm) is formed at the center of the subject's pupil, while an image of the uniformly illuminated first lens surface is formed at the subject's retina. The pupil image is formed 25 mm beyond the cube beamsplitter (BS).

A fraction (~50%) of the light scattered back out of the eye is reflected by the cube BS toward an eyepiece (EP). A white-light retinal image is formed for the operator. By placing a vertical polarizer after the lamp and a horizontal polarizer before the eyepiece, reflections from the cornea are greatly reduced, providing a high-contrast retinal image. Translating the eyepiece provides focus through a wide range of patient and operator refractive errors.

Intertwined with the retinal illumination/imaging subsystem is the laser delivery/collection subsystem. Any number of lasers can be coaligned and directed into the EOX prototype. For all of the animal data presented in this report, two astigmatically corrected diode lasers were used due to their portability and ruggedness. The two wavelengths used were 670 and 803 nm. The 670 nm laser is chosen as a wavelength at which the extinction coefficient of reduced hemoglobin is much greater than the extinction coefficient of oxygenated hemoglobin.²³ At 803 nm, the extinction coefficients of reduced hemoglobin and oxygenated hemoglobin are nearly the same. A galvanometer scanning mirror (SM) that is conjugate to the patient's pupil is used to scan the laser beams. The beams pivot about the center of pupil of the eye (25 mm beyond the cube BS). The beams are focused to a point at the subject's retina, and scanned in a line approximately 400 μm in length. The cube BS directs a fraction of the laser light scattered back out of the eye to a silicon photodiode (PD) for detection. A cross-polarizer scheme is again used to minimize corneal reflections. A limitation of the current instrument is that no means of adjusting laser collimation to accommodate for patient refractive errors exists. However, the beams entering the eye are only 1.25 mm in diameter, providing a very large depth of field. We have had little difficulty acquiring high spatial resolution scans in each of the swine tested

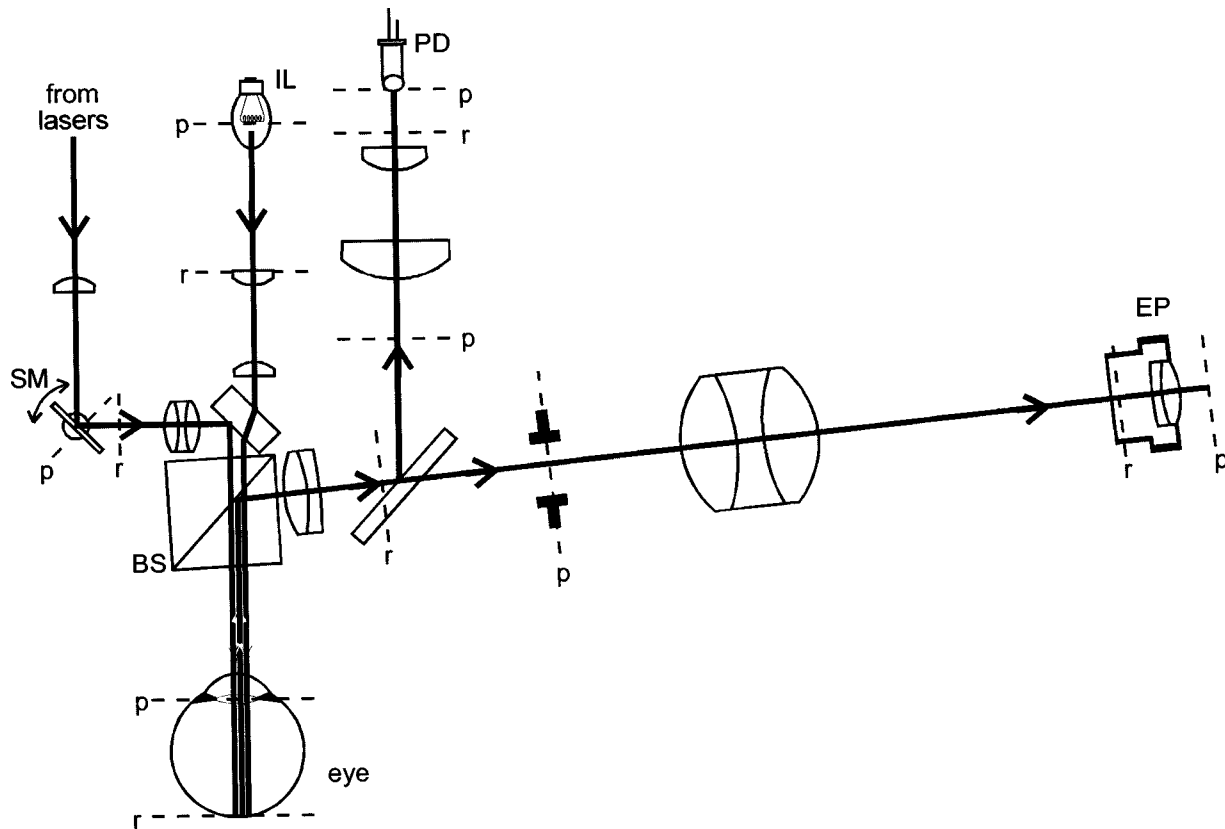


Fig. 1 Schematic of the eye oximeter prototype. Planes marked *p* are conjugate with the patient's pupil, and planes marked *r* are conjugate with the patient's retina.

with this device. Future versions of the EOX will provide focusing ability to the lasers, allowing high spatial resolution scans across a wide range of subject refractive errors.

The measurement sequence involves illuminating a spot on the retina with each of the lasers in turn, and measuring the returned flux from each laser. The signals from PD are digitized with a 14-bit analog-to-digital converter and uploaded to a laptop computer. The scanning mirror is then moved to the next scan location and each of the lasers are again measured in sequence. The procedure is repeated 256 times. The resulting linear scan on the retina contains each of the laser wavelengths. This procedure requires ~ 0.1 s. Generally, eight such scans are made in sequence, resulting in eight individual scans for each of the lasers acquired in ~ 0.8 s. These scans are stored in the computer for post-processing.

To perform a measurement, an operator observes the subject's retina through the eyepiece and chooses a retinal artery or vein. Since the operator is directly observing a white-light retinal image, arteries and veins are easily distinguished by their color and size, and by comparison of the EOX image with the image provided by direct ophthalmoscopy. Once the intended vessel is targeted by cross hairs in the eyepiece, the operator initiates the scanning sequence. The operator is able to faintly see the eight consecutive laser scans across the vessel

(of the 670 nm laser), and can immediately compare this with the vessel profiles displayed graphically on the computer. If the vessel profiles are visible in the scans, the data are saved for later analysis. If the vessel is missed (due to misalignment, eye motion, severe corneal glints, etc.), then the measurement is immediately repeated by the operator.

Since the eye oximeter shines lasers directly into a subject's eye, it is of utmost importance that the laser power levels are at or below safe levels. All laser safety considerations for the eye oximeter are derived from 21 CFR 1040.10, in the Code of Federal Regulations.²⁴ All laser products with viewports that allow direct retinal exposure to laser radiation must limit the level of laser radiation to less than the emission limits of class I. Class I levels of laser radiation are not considered to be hazardous. In all cases, the maximum permissible laser exposure is calculated assuming a failure mode of the EOX not scanning (i.e., a single retinal location illuminated continuously throughout an experiment). The lasers in the EOX were set to $\sim 130 \mu\text{W}$. This is approximately one-tenth of the class I limit, given the modulation frequency, duty cycle, scan time, and experiment length used by the EOX.

Additionally, the white-light exposure level is set to a retinal irradiance less than 1.4 mW cm^{-2} . This exposure level is not uncomfortable to a subject in a

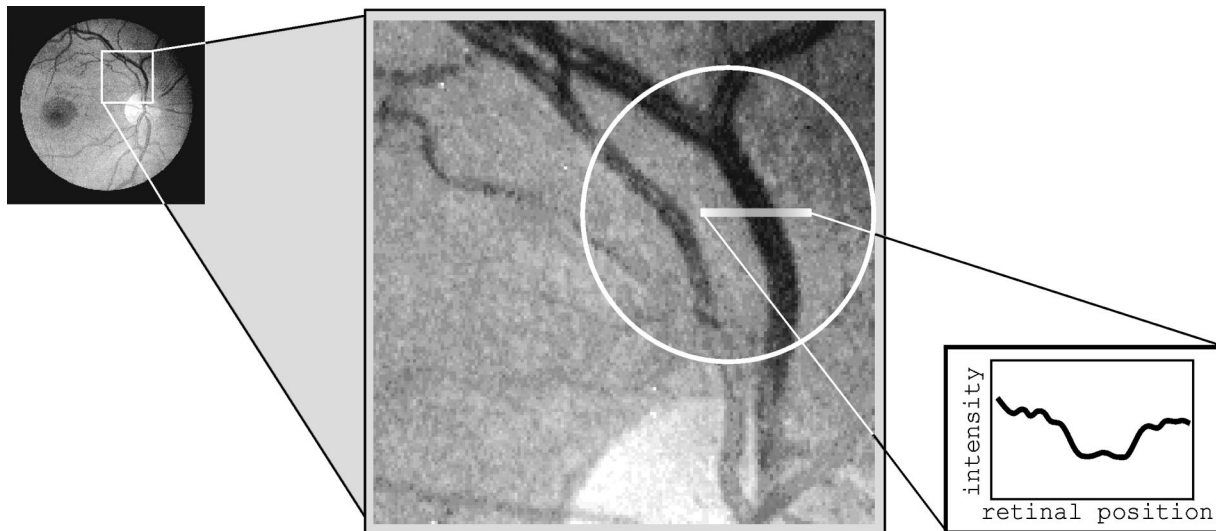


Fig. 2 Illustration of the signals collected by the eye oximeter. The white circle represents the field of view observable by the operator. The white line represents the length of a retinal scan (about $400\ \mu\text{m}$). The graph is the one-dimensional vessel absorption profile that is analyzed to determine the percent transmittance of the blood within the vessel.

darkened room. The maximum exposure time for this irradiance significantly exceeds the experiment time (about 1 min) that would be typical for human patients.²⁵

3 SIGNAL ANALYSIS AND DATA REDUCTION

Figure 2 illustrates the type of one-dimensional intensity profile that is measured when scanning a focused laser across a retinal blood vessel. The eye oximeter is generally used to measure the larger veins ($\sim 200\ \mu\text{m}$ diam) and arteries ($\sim 150\ \mu\text{m}$ diam) near the optic nerve head. The white circle in Figure 2 represents the size of the retinal image that the EOX operator observes. The white line is the approximate relative length of the laser scans. As seen in the graph in Figure 2, the collected intensity decreases as the scan crosses a vessel, and increases as the scan emerges from the opposite side of the vessel. Also note that there is generally a small increase in intensity at the center of the vessel. This increase is believed to be caused by the irregular specular reflections often observed along the apex of retinal vessels.²⁶

We believe that the vessel absorption profile in Figure 2 results from a complex combination of numerous light paths within the eye. There is light that is absorbed by the vessel, reflected from the underlying retinal layers, and absorbed again by the vessel in double pass. There is likely also light absorbed by the vessel, laterally diffused in the retinal layers, and scattered back out of the eye in single pass. Specular reflections from the inner limiting membrane, scattered light from red blood cells, and the absorption and scattering properties of vessel walls also influence the signal. As a final difficulty, the coloration of the retinal layers can vary significantly across the length of our retinal scans.

Efforts to incorporate each of the suspected light paths into our analysis are underway. However, in the analysis that follows we assume that the observed optical density of a vessel obeys Lambert-Beer's law. That is, the optical density is linearly related to both the thickness and the concentration of the medium. The optical density D of a vessel is, therefore, assumed to be described by

$$D = s\epsilon_{\text{HbO}_2}cl + (1-s)\epsilon_{\text{Hb}}cl, \quad (1)$$

where $D = -\log(T)$, T is the measured transmittance of the vessel, s is the oxygen saturation of the blood, c is the total hemoglobin concentration of the blood, l is optical path length, and ϵ_{Hb} and ϵ_{HbO_2} are the millimolar extinction coefficients of reduced hemoglobin and oxy-hemoglobin, respectively.²⁶ By measuring D at two wavelengths, Eq. (1) is easily solved for oxygen saturation s :

$$s = \frac{D^{\lambda_2}\epsilon_{\text{Hb}}^{\lambda_1} - D^{\lambda_1}\epsilon_{\text{Hb}}^{\lambda_2}}{D^{\lambda_1}(\epsilon_{\text{HbO}_2}^{\lambda_2} - \epsilon_{\text{Hb}}^{\lambda_2}) - D^{\lambda_2}(\epsilon_{\text{HbO}_2}^{\lambda_1} - \epsilon_{\text{Hb}}^{\lambda_1})}. \quad (2)$$

Note that Eqs. (1) and (2) assume Beer's law is valid in whole blood, which is not the case due to scattering caused by red blood cells. Previous studies^{21,22} have applied multiple scattering theory²⁷ to retinal vessel oximetry; however, it is not clear that this theory was well suited to the specific geometry of retinal vessels. While the Beer's law assumption in this study has produced encouraging results at 670/803 nm, we are continuing our work developing improved models that will improve the accuracy and precision of retinal oximetry.

Figure 3 illustrates the technique used to determine the percent transmittance of a vessel. This method performs curve fits to compensate for reflections from the vessel center, and for variation in retinal pigmentation. A line is calculated that connects the edges of the vessel profile (where the vessel slope approaches zero). This line estimates what the collected intensity of the retinal background would have been in the absence of the vessel. A cubic function is then linearly fitted to the vessel data. Only the data points within small regions centered on the slope extrema are used in the fit calculation. This cubic function estimates the depth of the absorption profile in the absence of the central glint. Dividing the vessel curve by the background line, and finding the minimum of this ratio, gives an estimate of the percent transmittance of blood within the vessel. This percent transmittance is the physical measurement made by the eye oximeter.

For a single oxygen saturation calculation, eight scans of each wavelength are acquired and analyzed as described above. The measured transmittance values are averaged to obtain a single transmittance value T for each wavelength. The transmittance values are converted into optical densities via the equation $D = -\log(T)$. Equation (2) is then used to calculate the oxygen saturation. Finally, the standard deviations of the transmittances are propagated through Eq. (2) to determine the uncertainty in the saturation calculation.

4 ARTERIAL CALIBRATION DATA

To establish the oxygen sensitivity of the eye oximeter, a series of arterial calibration experiments were performed in anesthetized swine.¹⁹ Swine were chosen for these studies due to similarity between swine and human retinal vasculature,²⁸ and because they provided a good cardiovascular model for blood loss studies. All animal protocols described in this report were approved by the Institutional Animal Care and Use Committee (IACUC) of The University of Alabama at Birmingham. All Public Health Services (PHS) guidelines regarding the care and use of laboratory animals were followed.

Seven young, female swine (18–32 kg) were used in this experiment. The 18 kg animal was excluded from this protocol because its retinal arteries were too small for analysis (see Sec. 6). The swine were placed in the supine position, intubated endotracheally, and placed on a ventilator. The swine were put on 2%–4% isoflurane anesthesia during surgical procedures. A femoral cut down was performed, and the femoral artery and vein were accessed. A maintenance solution of 5% dextrose in half normal saline with 10 mEq/L of KCl was infused intravenously at 80–110 mL/h. A fiber optic mixed venous oxygen saturation catheter was placed in the pulmonary artery (which contains venous blood) via the femoral vein. (This catheter was used for the

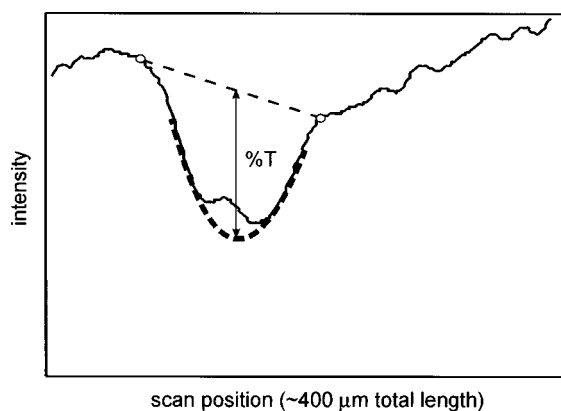


Fig. 3 Vessel profile analysis technique used to analyze the raw data. This method performs curve fits to compensate for vessel-center reflections and variations in fundus pigmentation. The transmittance of the blood within the vessel is calculated from the ratio of these curves.

blood loss study described in the next section.) When needed, arterial blood samples were drawn from the femoral artery. Blood samples were measured using an IL 482 CO-Oximeter system. Once the surgical preparation was completed, isoflurane was maintained at 1.25%–2% as needed to maintain anesthesia. The respiratory rate was adjusted to maintain arterial CO₂ tension between 36 and 44 mm Hg, and blood Ph between 7.35 and 7.45.

During the surgical preparation, the eyes of the swine were dilated using two drops of 1% cyclopentolate. The eyelids were then sutured open, and one or two sutures were placed in the conjunctiva to prevent the eye from drifting during the experiment. In order to reduce corneal stresses and irregularities that can cause significant optical aberrations, these sutures were placed as far from the cornea as possible, and as few sutures as possible were used. Once sutured open, the eye was bathed with 0.9% saline at least every 45 s to prevent corneal dehydration. The EOX was positioned, and the white-light image of the retina provided to the operator allowed selection of arteries or veins by direct observation of color (veins are darker) and size (veins are larger). The instrument was aimed at a large artery near the optic disk.

To perform this calibration study, the arterial saturation of the swine was varied via graded hypoxia. The oxygen was decreased incrementally from 100% to 7%. At each increment, the EOX scanned a large retinal artery, and samples drawn from the femoral artery were measured on the CO-Oximeter system. Retinal arterial oxygen saturation was calculated from the EOX scans in the method described in the previous section.

Figure 4 displays the correlation between femoral artery saturation and retinal artery saturation in a single swine. Error bars on this graph represent the standard error of each calculated saturation (derived from the eight EOX scans). Strong correlation

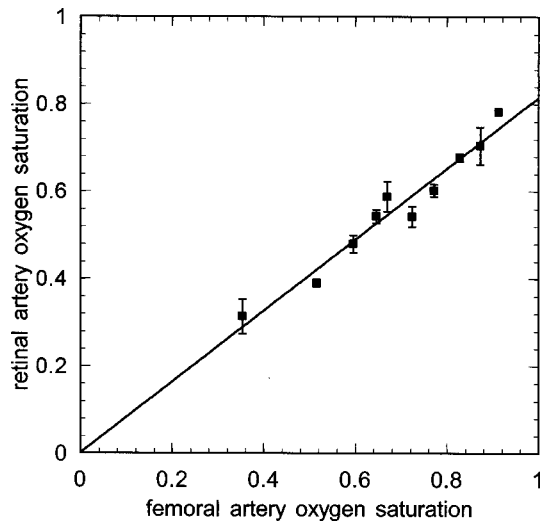


Fig. 4 Arterial calibration line from a single swine. The correlation between retinal arterial oxygen saturation (measured with the EOX) and femoral arterial oxygen saturation was very strong ($r^2 = 0.956$, $p < 0.001$). Error bars are standard error of the mean.

($r^2 = 0.956$, $p < 0.001$) was found between the two measurements. This calibration line has a slope of 0.81, and a y intercept of 0.0012.

This experiment was performed on all six swine. Table 1 summarizes the calibration lines calculated in each of these experiments. As demonstrated by the consistently high correlation values, the EOX measurements are able to follow saturation trends within a single animal. There is, however, variation in the slopes and y intercepts of these lines. Figure 5 contains plots of all six calibration lines. The average of the slopes of these six lines was $m = 0.80 \pm 0.11$, and the average y intercept was $b = 0.06 \pm 0.17$. From Figure 5 it is seen that four of the lines fell quite close together, while two had large differences in their y intercept. One of our current research efforts includes determining the cause of this variation and working to reduce it.

Table 1 Eye oximeter arterial calibration line data from six swine. The data from subject 4 are shown in Figure 4. The six calibration lines are plotted individually in Figure 5.

Subject	Slope	y intercept	r^2	Number of data points
1	0.734	0.160	0.957	6
2	0.812	0.100	0.897	7
3	0.831	0.770	0.998	6
4	0.814	0.001	0.956	10
5	0.976	-0.237	0.800	7
6	0.696	0.200	0.979	5

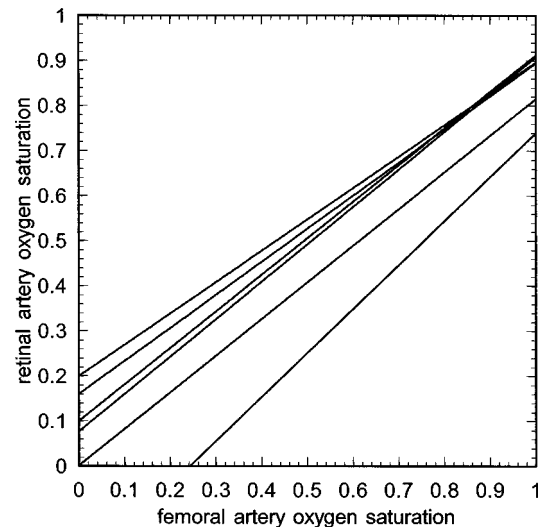


Fig. 5 Arterial calibration lines from six different swine. These lines illustrate the inter-animal variability of the EOX calibration.

5 BLOOD-LOSS DATA

A series of exsanguination studies were performed in anesthetized swine to determine if the eye oximeter can detect ongoing blood loss.¹⁹ Mixed venous oxygen saturation (measured in the pulmonary artery) is known to decrease predictably during blood loss.¹ As blood volume decreases, the body's oxygen carrying capacity decreases. As a result, a higher percent of O_2 is extracted at the end-body level (i.e., at the pulmonary artery). Unfortunately, making mixed venous saturation measurements requires catheterizing the heart, thus precluding this measurement during the early stages of trauma. It has been hypothesized that retinal venous saturation ($SrvO_2$) may also decrease predictably during blood loss.¹⁶ A primary motivation for developing the eye oximeter has been to investigate this hypothesis.

Seven young, female anesthetized swine were used in this study. The surgical preparation described in the previous section was performed. The EOX was positioned and aimed at a large retinal vein near the optic disk.

The swine were placed on 21% oxygen and bled at a controlled rate of approximately 0.5% of total blood volume every minute. This was continued for 40 min, resulting in a 20% blood loss. Throughout the experiment, mixed venous oxygen saturation was measured via a fiber optic Swan-Ganz catheter placed in the pulmonary artery. The eye oximeter scanned the retinal vein every 2 min throughout the experiment. Retinal venous oxygen saturation ($SrvO_2$) was calculated as described in Sec. 3. The $SrvO_2$ calculations in this section have not been adjusted based on the arterial calibration study in Sec. 4, and are therefore not expected to be well calibrated.

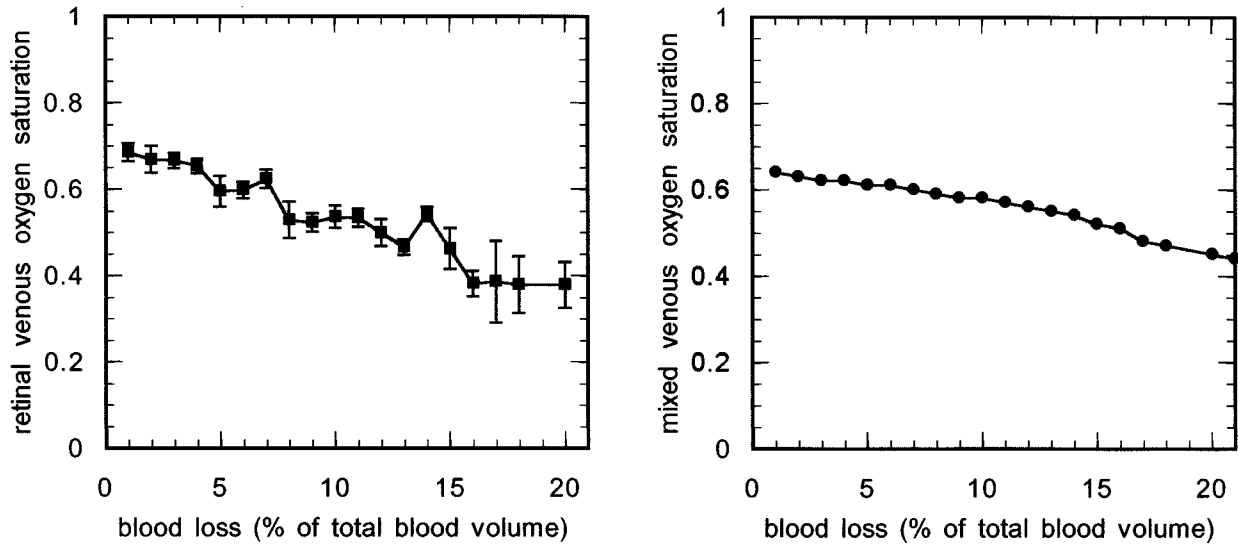


Fig. 6 Retinal venous oxygen saturation and mixed venous oxygen saturation both decrease with blood loss. These data are from a single swine, bled at a rate of 0.5% of total blood volume per minute. Error bars on the retinal saturations indicate uncertainty in the calculated oxygen saturation made with the eye oximeter.

The data in Figure 6 were collected from a single swine. As expected, mixed venous saturation measured with the pulmonary catheter decreases predictably with blood loss ($r^2=0.96$, $p<0.001$). Retinal venous saturation also correlates strongly with blood loss ($r^2=0.93$, $p<0.001$). The error bars on the $SrVO_2$ values indicate the standard error of the calculated saturation mean due to measurement variability in the eight EOX scans comprising each data point.

Figure 7 contains the results of averaging all seven swine in this study. In Figure 7, the error bars are the standard deviation of the population mean (note that to avoid overlap, only one half of each error bar is plotted). Since the calibration of the pul-

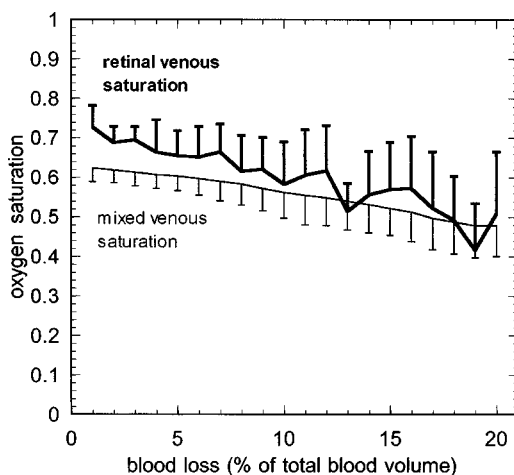


Fig. 7 The average results of seven swine are shown. Both mixed venous oxygen saturation and retinal venous oxygen saturation are found to correlate strongly with blood loss. The error bars represent standard deviations between subjects. (Note that only one half of each error bar is drawn in order to prevent overlap.)

monary catheter was verified prior to each use, the variability in the mixed venous saturation is expected to be a result of physiologic variability between animals. In addition to physiologic variability, the retinal venous saturation is also likely affected by the interanimal calibration variability observed in the arterial calibration experiment.

The average mixed venous saturation values correlate strongly ($r^2=0.96$, $p<0.001$) with blood loss. In addition, the average retinal venous saturation values, as measured with the EOX, are found to correlate strongly ($r^2=0.86$, $p<0.001$) with blood loss.

6 DISCUSSION AND CONCLUSIONS

We have established the feasibility of making fast, precise measurements of the oxygen saturation of blood within the large veins and arteries of the retina. Our arterial calibration lines were each found to be strongly linear; however, variations in the slopes and intercepts of these lines were observed. It is unclear whether this variation is an instrumental effect, a physiologic effect, or a combination of the two. Improved models of the light-vessel interaction, the incorporation of additional wavelengths, and an *in vitro* calibration study may lead to a more consistent intersubject calibration.

Our pilot animal data suggest that retinal venous saturation may be a sensitive indicator of blood loss. Retinal venous oxygen saturation measured with the eye oximeter decreased predictably as blood volume decreased. This resulted from proportionally more oxygen being extracted at the capillary beds as the bleeding ensued. However, this study was performed in anesthetized swine, and the response of retinal venous saturation to blood loss may be different in human trauma victims.

The red and near-infrared wavelengths used in the EOX restrict its use to retinal vessels larger than about 50 μm in diameter. Vessels smaller than 50 μm typically absorb less than 3% of the incident light at our wavelengths. This low absorbance makes vessel identification difficult, and results in large variations in the calculated saturation. The use of more highly absorbed wavelengths would allow the EOX to be tuned for these smaller vessels. In one of the swine used in this study, no retinal artery greater than 50 μm was present and the arterial calibration protocol could not be performed. This limitation may also prevent the use of the EOX (in its current configuration) on small children.

In this study, we sutured the anesthetized animals' eyes open and irrigated the cornea because the animals could not cooperate with an ophthalmic examination. Cooperative human patients will not require these measures. However, a method for immobilizing the eye or a complex tracking system would be required for uncooperative or unconscious patients, and use of the EOX on combative patients presents significant difficulties. The eyes of the swine in this study were dilated to facilitate alignment of the EOX. The eyes of human patients can generally be scanned by the EOX without dilation, unless their pupil diameter is less than about 2 mm. Finally, because of the need for a clear retinal image, the EOX may not be useful in patients with cataracts or corneal opacities. Despite these limitations, the EOX technology is noninvasive, and monitoring retinal versus saturation as an indicator of occult bleeding appears promising and warrants further investigation.

Acknowledgments

This work was supported by grants from The University of Alabama in Huntsville and The University of Alabama at Birmingham, and by a contract from Vectranetics, Inc. (Madison, AL 35899).

REFERENCES

1. T. M. Scalea, M. Holman, M. Furtes, B. J. Baron, T. F. Phillips, A. S. Goldstein, S. I. A. Sclafani, and G. W. Shaftan, "Central venous blood oxygen saturation: An early, accurate measurement of volume during hemorrhage," *J. Trauma* **28**(6), 725-732 (1988).
2. C. J. Wo, W. C. Shoemaker, P. L. Appel, M. H. Bishop, H. B. Kram, and E. Hardin, "Unreliability of blood pressure and heart rate to evaluate cardiac output in emergency resuscitation and critical illness," *Crit. Care Med.* **21**(2), 218-223 (1993).
3. G. K. Luna, A. C. Eddy, and M. Copass, "The sensitivity of vital signs in identifying major thoracoabdominal hemorrhage," *Am. J. Surg.* **157**, 512-515 (1989).
4. T. M. Scalea, R. W. Hartnett, A. O. Duncan, N. A. Atweh, T. F. Phillips, S. J. Sclafani, M. Fuortes, and G. W. Shaftan, "Central venous oxygen saturation: A useful clinical tool in trauma patients," *J. Trauma* **30**(12), 1539-1543 (1990).
5. T. M. Scalea, H. M. Simon, A. O. Duncan, N. A. Atweh, S. J. Sclafani, T. F. Phillips, and G. W. Shaftan, "Geriatric blunt multiple trauma: Improved survival with early invasive monitoring," *J. Trauma* **30**, 129-136 (1990).
6. B. Abou-Khalil, T. M. Scalea, S. Z. Trooskin, S. M. Henry, and R. Hitchcock, "Hemodynamic responses to shock in young trauma patients: Need for invasive monitoring," *Crit. Care Med.* **22**, 633-639 (1994).
7. C. D. Kurth, J. M. Steven, D. Benaron, and B. Chance, "Near infrared monitoring of the cerebral circulation," *J. Clin. Monit.* **9**, 163-170 (1993).
8. S. C. Dronen, P. A. Maningas, and R. Fouch, "Transcutaneous oxygen tension measurements during graded hemorrhage and reinfusion," *Ann. Emerg. Med.* **24**, 534-539 (1984).
9. M. Klein, D. Hess, D. Eitel, D. Bauernshub, and N. Sabulsk, "Conjunctival oxygen tension monitoring during controlled phlebotomy," *Am. J. Emerg. Med.* **6**, 11-13 (1988).
10. E. Abraham, "Conjunctival oxygen tension monitoring," *Int. Anesthesiol. Clin.* **25**(3), 97-112 (1987).
11. K. R. Denninghoff, M. H. Smith, R. A. Chipman, L. W. Hillman, P. M. Jester, F. Kuhn, D. Redden, and L. W. Rue, "Retinal venous oxygen saturation correlates with blood volume," *Acad. Emerg. Med.* (to be published).
12. A. Harris, O. Arend, K. Kopecky, K. Caldemeyer, S. Wolf, W. Sponsel, and B. Martin, "Physiological perturbation of ocular and cerebral blood flow as measured by scanning laser ophthalmoscopy and color Doppler imaging," *Surv. Ophthalmol. (Suppl.)* **38**, S81-S86 (1994).
13. M. Laughlin, W. M. Harold, and R. N. Whittaker, "Regional cerebral blood flow in conscious miniature swine during high sustained +G_z acceleration stress," *Aviat. Space Environ. Med.* **50**(11), 1129-1133 (1979).
14. A. Ames, "Energy requirements of CNS cells as related to their function and to their vulnerability to ischemia: A commentary based on studies on retina," *Can. J. Physiol. Pharmacol.* **70**, S158-S164 (1992).
15. T. E. Minnich, "Method and apparatus for monitoring the arteriovenous oxygen difference from the ocular fundus via retinal venous oxygen saturation," U.S. Patent No. 5,308,919 (1994).
16. T. E. Minnich, "Method and apparatus for monitoring blood loss via retinal oxygen saturation," U.S. Patent No. 5,119,814 (1992).
17. L. W. Hillman, S. C. McClain, M. H. Smith, and R. A. Chipman, "Eye oximeter for the noninvasive measurement of cardiac output," in *Vision Science and its Applications*, 1994 Technical Digest Series, Vol. 2, pp. 151-154, Optical Society of America, Washington DC (1994).
18. M. H. Smith, K. R. Denninghoff, L. W. Hillman, C. E. Hughes, T. E. Minnich, and R. A. Chipman, "Technique for noninvasive monitoring of blood loss via oxygen saturation measurements in the eye," *Proc. SPIE* **2982**, 46-52 (1997).
19. K. R. Denninghoff, M. H. Smith, R. A. Chipman, L. W. Hillman, P. M. Jester, C. E. Hughes, F. Kuhn, and L. W. Rue, "Retinal large vessel oxygen saturation correlates with early blood loss and hypoxia in anesthetized swine," *J. Trauma* **43**(1), 29-34 (1997).
20. J. B. Hickam, R. Frayser, and J. C. Ross, "A study of retinal venous blood oxygen saturation in human subjects by photographic means," *Circulation* **27**, 375-385 (1963).
21. A. J. Cohen and R. A. Laing, "Multiple scattering analysis of retinal blood oximetry," *IEEE Trans. Biomed. Eng.* **23**(5), 391-400 (1976).
22. F. C. Delori, "Noninvasive technique for oximetry of blood in retinal vessels," *Appl. Opt.* **27**(6), 1113-1125 (1988).
23. O. W. Van Assendelft, *Spectrophotometry of Haemoglobin Derivatives*, Charles C. Thomas, Springfield, IL (1970).
24. *Code of Federal Regulations*, Title 21, Food and Drugs, Part 1040.10, Performance Standards for Light-Emitting Products, laser products, U.S. Government Printing Office (1994).
25. F. C. Delori, J. S. Parker, and M. A. Mainster, "Light levels in fundus photography and fluorescein angioplasty," *Vision Res.* **20**, 1099 (1980).
26. F. C. Delori, E. S. Gragoudas, R. Francisco, and C. Pruett, "Monochromatic ophthalmoscopy and fundus photography," *Arch. Ophthalmol.* **95**, 861-868 (1977).
27. V. Twersky, "Absorption and multiple scattering by biological suspensions," *J. Opt. Soc. Am.* **60**, 1084-1093 (1970).
28. L. De Schaeppdrijver, P. Simoens, L. Pollet, H. Lauwers, and J. De Lay, "Morphologic and clinical study of the retinal circulation in the miniature pig. B: Fluorescein angiography of the retina," *Exp. Eye Res.* **54**, 975-985 (1992).